Chinese Chemical Letters 35 (2024) 108464

Contents lists available at ScienceDirect

Chinese Chemical Letters

journal homepage: www.elsevier.com/locate/cclet

Design, synthesis, and biological evaluation of 1,2,4-triazole derivatives as potent antitubercular agents

Yu Wen[a,1], Shichun Lun[b,1], Yuxue Jiao[a,1], Wei Zhang[a], Tianyu Hu[c], Ting Liu[a], Fan Yang[a], Jie Tang[d], Bing Zhang[c], William R. Bishai[b,*], Li-Fang Yu[a,*]

[a] *Shanghai Engineering Research Center of Molecular Therapeutics and New Drug Development, School of Chemistry and Molecular Engineering, East China Normal University, Shanghai 200062, China*
[b] *Center for Tuberculosis Research, Department of Medicine, Division of Infectious Disease, Johns Hopkins School of Medicine, Baltimore, MD, 21231-1044, United States*
[c] *Shanghai Institute for Advanced Immunochemical Studies and School of Life Science and Technology, ShanghaiTech University, Shanghai 201210, China*
[d] *Shanghai Key Laboratory of Green Chemistry and Chemical Process, School of Chemistry and Molecular Engineering, East China Normal University, Shanghai 200062, China*

ARTICLE INFO

Article history:
Received 17 January 2023
Revised 12 April 2023
Accepted 17 April 2023
Available online 18 April 2023

Keywords:
Tuberculosis
MDR and XDR-TB
MmpL3 inhibitor
1,2,4-Triazole
Structure-based drug design

ABSTRACT

Inhibition of mycobacterial membrane protein large 3 (MmpL3) thereby affecting the mycolic acid biosynthetic pathway has been proven to be an effective strategy for developing antitubercular drugs. Based on the X-ray crystal structure of MmpL3 inhibitor complexes, a series of novel 1,2,4-triazole derivatives were designed, synthesized and evaluated antitubercular activity against *Mtb* strain H37Rv. Comprehensive structure–activity relationship exploration resulted in the identification of compounds **21** and **28**, which possess potent antitubercular activity against *Mtb* strain H37Rv [minimum inhibitory concentration (MIC) = 0.03–0.13 μg/mL] and the clinical isolates of multidrug resistance (MDR) and extensive drug resistance (XDR) tuberculosis (MIC = 0.06–1.0 μg/mL). Moreover, compounds **21** and **28** showed neglectable cytotoxicity ($IC_{50} \geq 32$ μg/mL) to the mammalian Vero cells and favorable physicochemical and pharmacokinetic properties according to the *in silico* absorption, distribution, metabolism and excretion (ADME) prediction. Finally, the potential target of representative 1,2,4-triazole **28** was identified to be MmpL3 using a microscale thermophoresis (MST) assay.

Tuberculosis (TB) is a chronic infectious disease caused by *mycobacterium tuberculosis* (*Mtb*), which seriously endangers human health. The corona virus disease 2019 (COVID-19) pandemic has reversed years of global progress in tackling TB. TB deaths have increased for the first time in over a decade, according to the World Health Organization's (WHO) 2022 Global TB report [1]. In 2021, TB was the 13th leading cause of death globally, falling to the second place as a single cause but still accounting for about 1.6 million deaths, including 187,000 human immunodeficiency virus (HIV) positive cases, demonstrating that TB remains the most prevalent and deadly epidemic globally. Currently, the standard treatment for TB generally requires at least a six to nine months regimen of four first-line drugs to ensure complete eradication of TB. However, multidrug resistance (MDR) and extensive drug resistance (XDR) TB patients required a combination of more than seven antibiotics for more than 18 months, and the success rate of treatment was very limited [2,3]. An all-oral combination therapy consisting of recently approved antitubercular drugs (bedaquiline, pretomanid, and linezolid) was proposed at the Meeting on Combating Drug Resistance-Innovative TB Chemotherapy Plans organized by the TB Alliance. The research results showed that after six months of treatment, patients with drug-resistant TB had a success rate of 90% [4]. However, bedaquiline resistance has already emerged in a high TB burden country [5]. Developing antitubercular drugs with novel scaffolds and distinct mechanisms of action is of substantial significance for the clinical treatment of drug-resistant TB.

Mycobacterial membrane protein large (MmpL) is a group of membrane proteins encoded by the *Mycobacterium* genome, which belongs to the resistance, nodulation, and cell division proteins (RND) family, and has 13 subtypes [6]. All of them are involved in the relevant biological functions of mycobacterial cell membranes (play an essential role in the transport of lipids, polymers, and immunomodulators), and were found to rely on proton-motive

* Corresponding authors.
E-mail addresses: wbishai1@jhmi.edu (W.R. Bishai), lfyu@sat.ecnu.edu.cn (L.-F. Yu).
[1] These authors contributed equally to this work.

https://doi.org/10.1016/j.cclet.2023.108464
1001-8417/

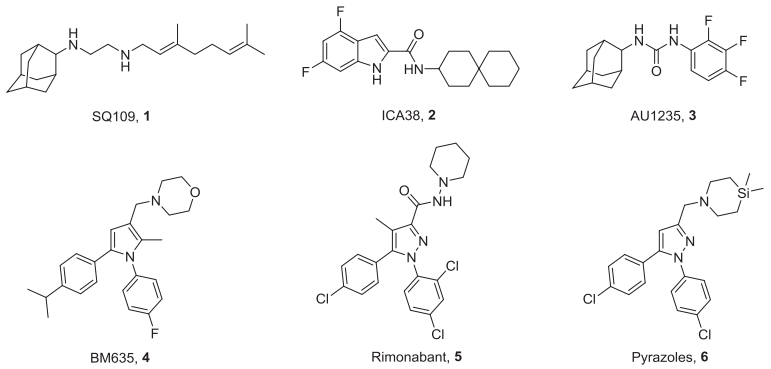

Fig. 1. Structures of representative MmpL3 inhibitors.

force (PMF) as the energy for substrate transport [7,8]. Among the 13 MmpL subtypes, MmpL3 is an essential transmembrane protein for bacterial cell replication and survival [9–11]. The *mmpL3* CRISPRi knockdown strain of *Mtb* had increased susceptibility to SQ109, a drug candidate against drug-resistant *Mtb* currently in Phase IIb/III clinical trials [12–15]. The sputum clearance rate of SQ109 for MDR-TB patients was similar to bedaquiline and delamanid. These studies further demonstrate the potential of MmpL3 as an antitubercular therapeutic target.

Several MmpL3 small-molecule inhibitors with different scaffolds have been reported (Fig. 1), including ethylenediamine (SQ109, **1**), indole-2-carboxamides (ICA38, **2**), adamantyl ureas (AU1235, **3**), pyrroles (BM635, **4**), and pyrazoles (rimonabant, **5** and **6**) [16–19]. Notably, compound **4** has potent *in vitro* antitubercular activities and is currently in preclinical evaluation [20–22]. Rimonabant is the first type 1 cannabinoid receptor (CB1) antagonist for weight loss. Interestingly, it has also been found to show inhibitory activity on MmpL3 [19]. SQ109 is considered an MmpL3 inhibitor; however, no resistant mutants of SQ109 have been directly isolated *in vitro* or *in vivo*. In addition, SQ109 was found to interfere with menaquinone biosynthesis and electron transport [23].

According to the four complexes structures of *mycobacterium smegmatis* (*Msmg*) MmpL3 and its inhibitors (SQ109, ICA38, AU1235, and rimonabant), the binding pocket consists of 5 binding regions (S1–S5) [16], including 4 hydrophobic regions S1 (V245, I319, V638), S2 (L686, V689, L708), S3 (V638, G641, L642), S5 (F260, S293, F649), and one hydrogen bonding region S4 (D645). All four inhibitors form an essential hydrogen bond with D645 blocking two pairs of Asp–Tyr-hydrogen bonds (Y256–D646; Y257–D645), thereby interfering with the proton transport function of MmpL3 (Fig. 2A). The five-membered aromatic heterocyclic module is a common structural unit in drugs, including the antituberculosis field [24], as it can form dipole-dipole and π-stacking interactions and hydrogen bonds, possibly improving the solubility and binding capacity of biological targets. *N*-Containing five-membered heterocyclic derivatives with better physicochemical properties were reported to have significant antibacterial (including antitubercular) activities, including pyrrole [25–28], pyrazole [19,29], and 1,2,4-triazole [30–33] skeletons. The triazole heterocycles have been considered one of the most valuable scaffolds in drug discovery and development [34,35], and the 1,2,4-triazole structural unit processes relatively high calculated Log*S* value (−0.1254) compared to other heterocycles, *e.g.* pyrrole (Log*S*: −0.834) and pyrazole (Log*S*: −0.7903) (Fig. 2B). Herein, we present our design and development of a 1,2,4-triazole core containing MmpL3 inhibitors utilizing a structural-based approach. Compounds targeted to MmpL3 protein are generally lipophilic because of the hydrophobic nature of the binding site as aforementioned. However, too high cLog*P* may be deleterious as this will negatively impact aqueous solubility and plasma protein binding. Thus, we strive to balance lipid solubility and antitubercular activity during compound optimization. Structure–activity relationships (SARs) of *N*-heterocyclic (S5 region) and R^1 (S1 region) and R^2 (S2 region) were systematically explored.

Two synthetic routes were exploited to access desired 1,2,4-triazole derivatives **14**–**46** and **53**–**56** (Schemes 1 and 2). Compounds **14**–**46** were synthesized from commercially available 4-fluoroaniline **7** and cuminaldehyde **9** *via* five steps (Scheme 1). The key 1,2,4-triazole intermediate **11** was synthesized according to a previously reported paper [36]. 4-Fluoroaniline **7** was first converted to diazonium salt by the treatment with $NaNO_2$/HCl at 0 °C. Then the diazonium salt was reacted with methyl 2-chloroacetoacetate to give hydrazonoyl chloride **8**. Aldehyde **9** was converted to the oxime intermediate and underwent a 1,3-dipolar cycloaddition reaction with hydrazonoyl chloride **8** in the presence of Et_3N to obtain the key 1,2,4-triazole intermediate **11**. The 1,2,4-triazole **11** was further reduced and oxidized to the corresponding aldehyde **12** using sodium borohydride and Dess-Martin periodinane, respectively. Reductive amination of aldehyde **12** with various amines in the presence of sodium triacetoxyborohydride successfully obtained target compounds **14**–**41.** Hydrolysis of methyl ester **11** under basic conditions afforded carboxylic acid **13**, which was subjected to a subsequent amide condensation reaction with various amines to afford target compounds **42**–**46**.

The intermediate **48** was obtained *via* introducing a Cbz group and then interacted with 4-isopropylaniline to get intermediate **49** through the amide condensation reaction (Scheme 2). The Cbz protecting group of **49** was removed under the conditions of Pd/C and hydrogen to obtain the intermediate **50**, followed by a cycloaddition reaction with ethyl thiooxamate to get the 1,2,4-triazole **51**. The aldehyde **52** was synthesized *via* successively reduction and oxidation reactions using sodium borohydride and Dess-Martin periodinane, respectively. Finally, in the presence of sodium triacetoxyborohydride, intermediate **52** underwent reductive amination with 4,4-dimethylpiperidine or 4,4-dimethyl-1,4-azasilinane to obtain target compounds **55** or **56**. Similarly, compounds **53** and **54** were obtained from starting material isopropyl hydrazine.

All final compounds were initially evaluated for their minimum inhibitory concentration (MIC) values against the *Mtb* strain H37Rv in a standard microplate Alamar blue assay (MABA) [37,38]. The initial round of SAR modifications was focused on the substitutions on the 3-position of 1,2,4-triazole core (R^3 group), which presumably occupy the essential S1 hydrophobic pocket and forms an essential hydrogen bond with residue D645 of the MmpL3 protein. Poce *et al.* reported that the 4-fluorophenyl and 4-isopropylphenyl substituents attached to the pyrrole or pyrazole core could effectively occupy the S1 and S2 hydrophobic regions of MmpL3 [21,28]. Therefore, we first introduced

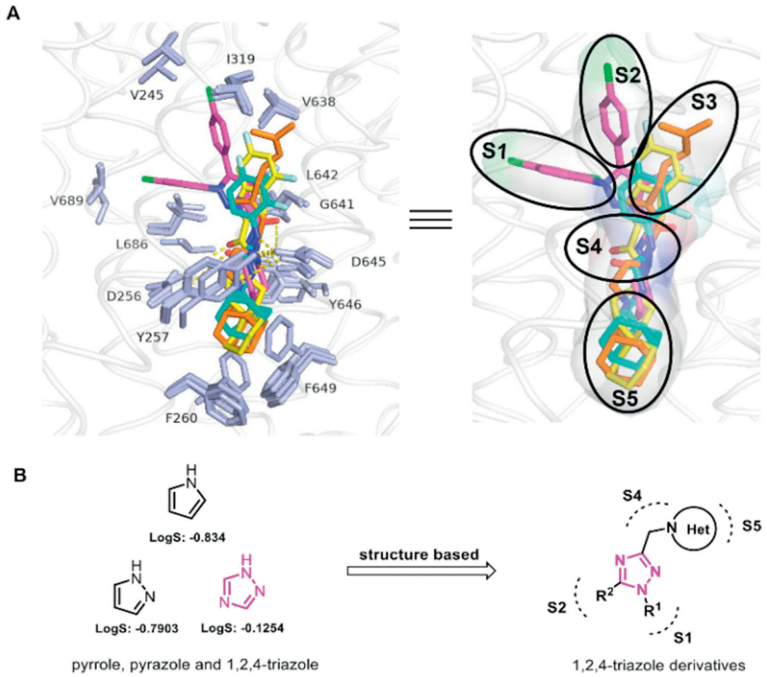

Fig. 2. (A) The binding pocket of MmpL3 with 4 representative inhibitors SQ109 (orange sticks, PDB: 6AJG), ICA38 (yellow sticks, PDB: 6AJJ), AU1235 (light blue sticks, PDB: 6AJH), and rimonabant (pink sticks, PDB: 6AJI). (B) Design of 1,2,4-triazole derivatives.

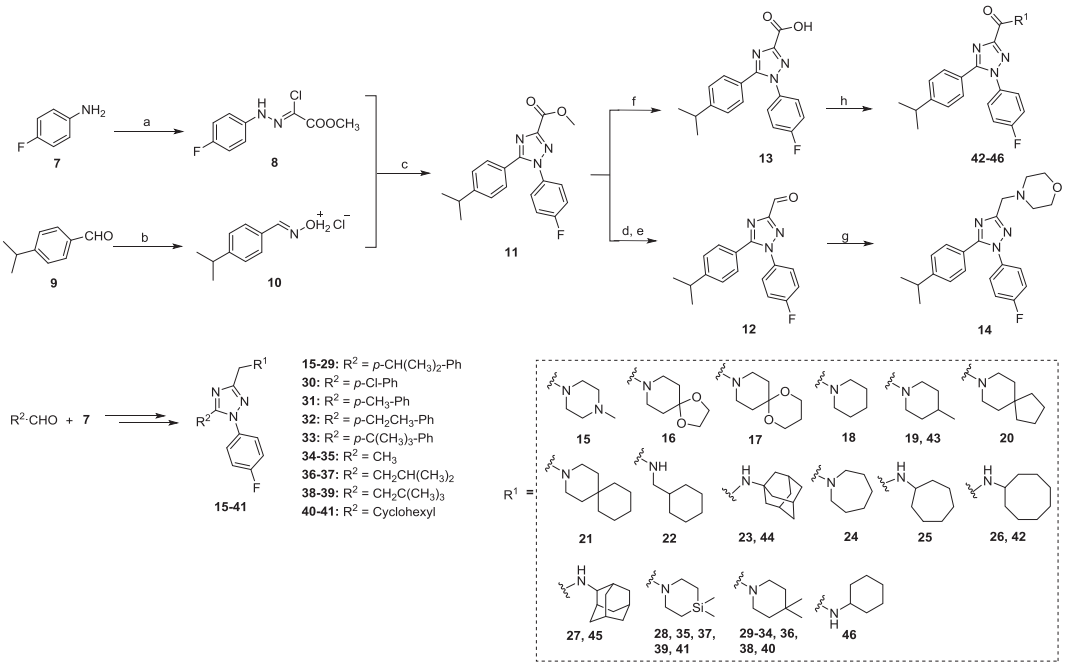

Scheme 1. Synthesis of 1,2,4-triazole derivatives **14–46**. Reagents and conditions: (a) (i) $NaNO_2$, 3 mol/L HCl (aq.), 0 °C, 1 h; (ii) methyl 2-chloroacetoacetate, AcONa, EtOH, r.t., 4 h; (b) $NH_2OH{\cdot}HCl$, PhMe, r.t., 0.5 h; (c) Et_3N, reflux, 1–2 h; (d) $NaBH_4$, MeOH, r.t., overnight; (e) Dess-Martin periodinane, CH_2Cl_2, r.t., 2 h; (f) LiOH, MeOH:THF:H_2O = 2:1:1, 50 °C, 3 h; (g) various amines, $NaBH(AcO)_3$, CH_2Cl_2, r.t., overnight; (h) various amines, EDCI, HOBt, DIPEA, CH_2Cl_2, r.t., 6 h.

these two substituents to the 1- and 5-positions (R^1 and R^2 groups) of the 1,2,4-triazole core. Various sterically hindered *N*-containing cyclics (*N*-morpholine, *N*-1-methylpiperazine, *N*-1,4-dioxa-8-azaspiro[4.5]decane, *N*-1,5-dioxa-9-azaspiro[5.5]undecane, *N*-piperidine, *N*-4-methylpiperidine, *N*-8-azaspiro[4.5]decane, *N*-3-azaspiro[5.5]undecan, *N*-cyclohexylmethanamine, *N*-1/2-amantadine, *N*-azepane, *N*-cycloheptylamine, and *N*-cyclooctylamine) were selected for R^3. As shown in Table 1, cyclic amines **19**–**27** generally showed moderate to good antitubercular activities with MIC values ranging from 0.0625 μg/mL to 4 μg/mL, except compound **18** (MIC = 16 μg/mL). Inserting N or O atoms into cyclic amines (**14**–**17**) resulting a decrease in activity (MIC = 0.5–64 μg/mL), suggesting that lipophilicity of the R^3 group is crucial. The increase in the steric effect of cyclic amine (**18**–**20**) is accompanied by an obvious improvement in activity. It is speculated that larger hydrophobic groups can insert deeply into the S5 hydrophobic pocket (F260, S293, F649). The spiroanalogues **20** and **21** were the most potent active compounds with MIC values of 0.0625–0.125 μg/mL. The bioisosteric replacement of a carbon atom with a silicon atom holds the potential to improve the properties

Table 1
The antitubercular activity of 1,2,4-triazole derivatives **14**–**29** and **42**–**46** against *Mtb* strain H37Rv.

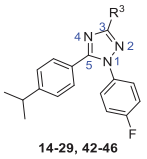

14-29, 42-46

Compd.	R^3	MIC (μg/mL)[a]	cLog*P*[b]	Compd.	R^3	MIC (μg/mL)[a]	cLog*P*[b]
14		64	4.62	**25**		4–8	6.84
15		32	5.07	**26**		1–2	7.39
16	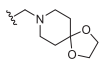	2	4.44	**27**	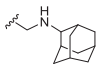	4	7.94
17		0.5	4.22	**28**	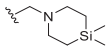	0.03125	8.51
18		16	5.90	**29**	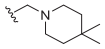	0.25	6.94
19		2	6.42	**42**		64	7.74
20	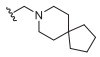	0.125	7.34	**43**		32	5.24
21	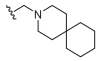	0.0625–0.125	7.89	**44**	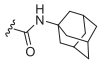	64	7.25
22	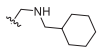	4	6.90	**45**	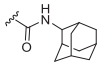	64	7.25
23	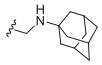	1	7.94	**46**	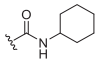	32	6.62
24		4	6.46				

[a] The lowest concentration of compounds leading to at least 90% inhibition of bacterial growth signal by MABA. MIC values are reported as an average of three individual measurements.
[b] cLog*P* was calculated using ChemBioDraw Ultra 16.0.

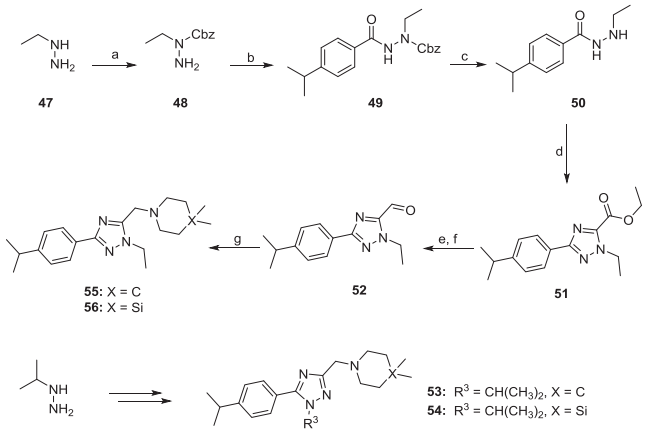

Scheme 2. Synthesis of 1,2,4-triazole derivatives **53–56**. Reagents and conditions: (a) Cbz-Cl, Et_3N, CH_2Cl_2, 0 °C, 3–4 h; (b) 4-propan-2-ylbenzoyl chloride, Et_3N, CH_2Cl_2, 0 °C–rt, 3–4 h; (c) 10% Pd/C, MeOH, H_2, r.t., overnight; (d) ethyl thiooxamate, PhMe:AcOH = 10:1, 90 °C, 10 h; (e) $NaBH_4$, MeOH, r.t., overnight; (f) Dess-Martin periodinane, CH_2Cl_2, r.t., 2 h; (g) dimethyl piperidine or 4,4-dimethyl-1,4-azasilinane, $NaBH(AcO)_3$, CH_2Cl_2, r.t., overnight.

of a compound and to create intellectual property space [39]. Ramesh *et al*. reported that the activity of *N*-4,4-dimethylazasilyl analogues was improved due to the enhancement of lipophilicity [19]. In our case, compound **28** (MIC = 0.03125 μg/mL) bearing an *N*-4,4-dimethylazasilyl moiety showed 8-fold more active than the corresponding *N*-4,4-dimethylpiperidine **29** (MIC = 0.25 μg/mL). Replacing amines with amides (**42**–**46**) resulted in inactivity due to the loss of the essential hydrogen bond with the carboxyl of D645.

Subsequent SAR investigation was focused on the 1- and 5-positions of 1,2,4-triazole core (R^1 and R^2 groups, Table 2). We introduced substituents at the *para* position of the phenyl group at the R^2 position to explore the electronic effects. The introduction of electron-donating groups (EWGs) such as methyl (**30**), ethyl (**31**), and *tert*–butyl (**32**) showed similar antitubercular activities (MIC = 0.25–1 μg/mL) to the 4-isopropyl **29** (MIC = 0.25 μg/mL). In the contrast, introducing an electron-withdrawing group (EWG; -Cl, compound **33**), resulted in a 32-fold reduction in activity, thus terminating further exploration of EWG. Replacing the substituted phenyl ring with aliphatic groups at the 1-position (-^{i}PrCH$_2$) or 5-position (-Me, -^{i}PrCH$_2$, -^{t}BuCH$_2$, cyclohexyl) of 1,2,4-triazole core decreased the antitubercular activity (compounds **34**–**41**, MIC = 1–64 μg/mL) compared to compounds **28** (MIC = 0.03125 μg/mL) and **29** (MIC = 0.25 μg/mL). These results suggest that higher lipophilic moieties at the R^1 or R^2 are more favorable in activity. Consistent with the trend in compounds **18**–**20**, the increase in the steric hindrance of the 1-position (-^{i}PrCH$_2$, 4-isopropylphenyl) and 5-position (-Me, -^{i}PrCH$_2$, -^{t}BuCH$_2$, cyclohexyl, 4-fluorophenyl) substituents was accompanied by an increase in antitubercular activity. Moving the alkyl substituent to the 2-*N* led to a significant loss of activity (**55** and **56**, MIC = 16 μg/mL).

We plotted the correlation between the antitubercular activity of triazole derivatives and cLog*P* values. As shown in Fig. S1 (Supporting information), the antitubercular activity of triazole compounds is positively correlated with the cLog*P* values. Compounds **21** and **28** exhibited the most potent antitubercular activity, ac-

Table 2
The antitubercular activity of 1,2,4-triazole derivatives **30–41** and **53–56** against *Mtb* strain H37Rv.

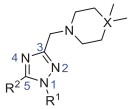
30-41, 53-54

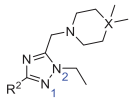
55-56

Compd.	R^1	R^2	X	MIC (μg/mL)[a]	cLog*P*[b]
30			C	1	6.01
31			C	0.25	6.54
32		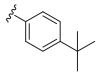	C	0.25	7.34
33			C	8	6.23
34		CH_3	C	>64	5.58
35		CH_3	Si	64	6.34
36			C	64	5.14
37			Si	16	6.71
38			C	32	5.54
39			Si	4	7.11
40			C	32	5.81
41			Si	1	7.37
53	$CH(CH_3)_2$		C	1	5.69
54	$CH(CH_3)_2$		Si	0.5	7.25
55	–		C	16	5.38
56	–		Si	16	6.94

[a] The lowest concentration of compounds leading to at least 90% inhibition of bacterial growth signal by MABA. MIC values are reported as an average of three individual measurements.
[b] cLog*P* was calculated using ChemBioDraw Ultra 16.0.

companied by the highest cLog*P* values. Compounds with higher lipophilicity showed more potent activity.

The active compounds with MIC values less than 1 μg/mL were selected to further evaluate their cytotoxicity profiles against Vero cells derived from African green monkey kidneys. A comparison of the Vero cell toxicity [half maximal inhibitory concentration (IC_{50}) values] and the MIC values for *Mtb* growth inhibition gives a measure of the general toxicity profile of the compound of interest [40]. As shown in Table 3, all tested compounds showed low cytotoxicity in Vero cells with IC_{50} values greater than 16 μg/mL. Notably, compounds **21** and **28** with the most potent antitubercular activity, showed neglectable cytotoxicity ($IC_{50} \geq 32$ μg/mL).

Compounds **21** and **28** obtained were antitubercular activity evaluated on susceptible-TB (V4207), MDR-TB (V2475 and KZN494), and XDR-TB (R506 and TF274) strains of clinical isolates [41]. First-line antitubercular drugs (isoniazid and rifampin) and second-line antitubercular drugs (levofloxacin, ofloxacin, and kanamycin) were used as a positive control (Table 4). To our delight, compounds **21** and **28** had equally potent activity against susceptible *Mtb* strains and all MDR and XDR clinical isolates tested. The high activities against the MDR and XDR-TB highlight the potential use of 1,2,4-triazole derivatives to treat drug-resistant *Mtb* and the likelihood that they will not exhibit cross-resistance with currently used medications.

Table 3
Vero toxicity of compounds **17**, **20**, **21**, **23**, **26**, **28–32**, **41**, **53**, and **54**.

Compd.	Vero cells IC_{50} (μg/mL)	MIC H37Rv[a] (μg/mL)
17	≥32	0.5
20	≥32	0.125
21	≥32	0.0625–0.125
23	≥32	1
26	16	1–2
28	≥32	0.03125
29	≥32	0.25
30	≥32	1
31	≥32	0.25
32	16	0.25
41	≥32	1
53	≥32	1
54	≥32	0.5

[a] The lowest concentration of compounds leading to at least 90% inhibition of bacterial growth signal by MABA. MIC values are reported as an average of three individual measurements.

Table 4
The antitubercular activity of compounds **21** and **28** against susceptible, MDR, and XDR strains of *Mtb*.

Strain/phenotype	*Mtb* MIC[d] (μg/mL)				
	V4207/ DS[a]	V2475/ MDR[b]	KZN494/ MDR[b]	R506/ XDR[c]	TF274/ XDR[c]
21	0.125	1	0.125	0.125	0.125
28	0.125	0.5	0.125	0.0625	0.0625
Isoniazid	0.04	16	16	8	8
Rifampin	0.0625	4	128	>128	>128
Levofloxacin	0.125	NT	NT	2	1
Ofloxacin	0.5	0.5	0.5	4	8
Kanamycin	2	2	2	>128	>128

[a] Drug susceptible strain of *Mtb*.
[b] Multidrug resistant strain of *Mtb*.
[c] Extensively drug resistant strain of *Mtb*.
[d] The lowest drug concentration leads to at least a 90% reduction of bacterial growth signal by MABA; reported MIC values are an average of three individual measurements.

The physicochemical properties of pyrazole/triazole-based derivatives **21**, **28**, and bedaquiline were predicted using ADMET Lab (Table S1 in Supporting information). The molecular weights and hydrogen-bond acceptor numbers of the three compounds are in accordance with Lipinski's rule of five (RO5). Compounds **21**, **28** and bedaquiline have similar antitubercular activity *in vitro*, but the Log*S* of 1,2,4-triazole derivatives **21** and **28** are lower than bedaquiline (Log*S*: −6.16, −5.97 *vs.* −8.79). Among them, compound **21** showed the lowest cLog*P* value of 7.90 similar to bedaquiline (cLog*P*: 7.25). The permeability coefficient (suggestion: >−5.15 cm/s) of Caco-2 monolayers (Papp) is commonly used to evaluate human intestinal permeability [42]. Compounds **21** and **28** have $\log_{10}$Papp values of −4.79 and −4.69, respectively, indicating that they have the potential to traverse the cell membranes. The predicted plasma protein binding (PPB) degrees of compounds **21** and **28** were 86.8% and 90.5%, suggesting that these compounds may have a long plasma half-life.

To investigate the binding mode of 1,2,4-triazole derivatives and MmpL3, we performed molecular docking studies with repre-

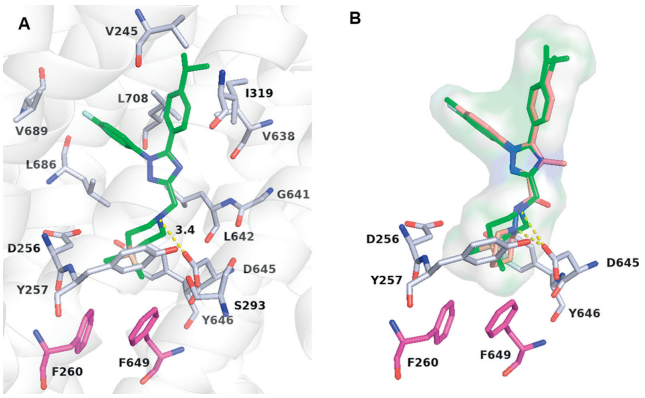

Fig. 3. (A) Proposed binding mode of compound **28** (green) with MmpL3 (PDB: 6AJI). (B) Superposed docking poses of **28** and rimonabant (orange).

sentative compound **28**. The crystal structure used was MmpL3-rimonabnt (PDB: 6AJI) [16], the docking calculation was carried out using the Schrödinger's Glide-XP module, and Pymol 2.5 was used for later protein and small molecule processing. Compound **28** successfully binds to the active pocket of MmpL3 (docking score = −13.19) located in the center of the MmpL3. As shown in Fig. 3A, the N atom of *N*-4,4-dimethylazasilyl and the carboxyl of residues D645 formed a key hydrogen bond (3.4 Å), which blocked the original hydrogen bond pairs (Y256–D646; Y257–D645) and affected the proton-motive force of MmpL3 protein. In addition, compound **28** also forms hydrophobic interactions with hydrophobic pockets of MmpL3, including *N*-4,4-dimethylazasilyl and residues F260, S293, F649; 4-fluorophenyl and residues V245, I319, V638; 4-isopropylphenyl and residues L686, V689, L708. A stacking docking study (Fig. 3B) showed that the binding modes of **28** and rimonabant were similar. However, the hydrophobic dimethyl moiety of **28** could insert more deeply into the hydrophobic region S5 (F260, F649) than the piperidinyl of rimonabant, leading to a more potent antitubercular activity.

Further, to verify the potential biding target of 1,2,4-triazoles compounds, we conducted a binding affinity study of representative compound **28** with *Msmg* MmpL3 using a microscale thermophoresis (MST) assay. As shown in Fig. S2 (Supporting information), **28** directly binds to *Msmg* MmpL3 with a K_d value of 25.2 μmol/L, which is slightly more potent than that of rimonabant (K_d = 29.5 μmol/L) [16].

Structure-based rational design and medicinal chemistry optimization focused on maximizing MmpL3 target occupancy led to the discovery of 1,2,4-triazole derivatives, a potent antitubercular agent effective against drug-susceptible/resistant mycobacteria. Representative compounds **21** and **28** showed the most potency against *Mtb* strain H37Rv with MIC values of 0.0312–0.125 μg/mL. The cytotoxic evaluations of compounds **21** and **28** to Vero cells showed the lowest toxicity ($IC_{50} \geq 32$ μg/mL). More importantly, compounds **21** and **28** had equally potent activities against the clinical isolates of MDR and XDR-TB, suggesting little cross-resistance with currently used medications. In comparison, compound **28** (cLog*P*: 8.51) exhibited a slightly higher cLog*P* value than **21** (cLog*P*: 7.89) due to the introduction of a lipophilic silicon atom. Furthermore, 1,2,4-triazoles **28** could directly bind to the *Msmg* MmpL3 in MST assay. Overall, these identified 1,2,4-triazole containing antitubercular compounds hold the promise for further lead optimization.

Declaration of competing interest

The authors declare that they have no known competing financial interests or personal relationships that could have appeared to influence the work reported in this paper.

Acknowledgments

This work has been supported by the National Natural Science Foundation of China (Nos. 82073706 and 22107031). This project has also been funded in part with Federal funds from the National Institutes of Health and National Institute of Allergy and Infectious Diseases, Department of Health and Human Services (No. AI155602).

Supplementary materials

Supplementary material associated with this article can be found, in the online version, at doi:10.1016/j.cclet.2023.108464.

References

[1] World Health Organization (2022). https://www.who.int/health-topics/tuberculosis#tab=tab_1.
[2] A.J. Nunn, P.P. Phillips, S.K. Meredith, et al., N. Engl. J. Med. 380 (2019) 1201–1213.
[3] J.C. Brust, N.R. Gandhi, S. Wasserman, et al., Clin. Infect. Dis. 73 (2021) 2083–2092.
[4] F. Conradie, A.H. Diacon, N. Ngubane, et al., N. Engl. J. Med. 382 (2020) 893–902.
[5] E. Chesov, D. Chesov, F.P. Maurer, et al., Eur. Respir. J. 59 (2022) 2100621.
[6] A. Viljoen, V. Dubois, F. Girard-Misguich, et al., Mol. Microbiol. 104 (2017) 889–904.
[7] J.A. Delmar, T.H. Chou, C.C. Wright, et al., J. Biol. Chem. 290 (2015) 28559–28574.
[8] R. Székely, S. Cole, Mol. Microbiol. 99 (2016) 831–834.
[9] J.M. Belardinelli, A. Yazidi, L. Yang, et al., ACS Infect. Dis. 2 (2016) 702–713.
[10] J.M. Belardinelli, C.M. Stevens, W. Li, et al., Sci. Rep. 9 (2019) 10728.
[11] W. Li, C.M. Stevens, A.N. Pandya, et al., ACS Infect. Dis. 5 (2019) 1001–1012.
[12] K.A. Sacksteder, M. Protopopova, C.E. Barry, et al., Future Microbiol. 7 (2012) 823–837.
[13] M.J. Boeree, N. Heinrich, R. Aarnoutse, et al., Lancet Infect. Dis. 17 (2017) 39–49.
[14] S. Borisov, E. Bogorodskaya, G. Volchenkov, et al., Tuberculosis Lung Dis. 96 (2018) 6–18.
[15] M.B. McNeil, G.M. Cook, Antimicrob. agents CH. 63 (2019) e00629-00619.
[16] B. Zhang, J. Li, X. Yang, et al., Cell 176 (2019) 636–648.
[17] M. Shao, M. McNeil, G.M. Cook, et al., Eur. J. Med. Chem. 200 (2020) 112390.
[18] M.D. Umare, P.B. Khedekar, R.V. Chikhale, ChemMedChem 16 (2021) 3136–3148.
[19] R. Ramesh, R.D. Shingare, V. Kumar, et al., Eur. J. Med. Chem. 122 (2016) 723–730.
[20] J. Stec, O.K. Onajole, S. Lun, et al., J. Med. Chem. 59 (2016) 6232–6247.
[21] G. Poce, M. Cocozza, S. Alfonso, et al., Eur. J. Med. Chem. 145 (2018) 539–550.
[22] M.S. Scherman, E.J. North, V. Jones, et al., Bioorg. Med. Chem. 20 (2012) 3255–3262.
[23] Z. Gil, N. Martinez-Sotillo, A. Pinto-Martinez, et al., Parasitol. Res. 119 (2020) 649–657.
[24] Z.J. Liu, X.Y. Guo, G. Liu, et al., Chin. Chem. Lett. 27 (2016) 51–54.
[25] M. Biava, G. Porretta, G. Poce, et al., J. Med. Chem. 49 (2006) 4946.
[26] G. Poce, R.H. Bates, S. Alfonso, et al., PLoS One 8 (2013) e56980.
[27] S. Bhakta, N. Scalacci, A. Maitra, et al., J. Med. Chem. 59 (2016) 2780–2793.
[28] H. Zhao, Y. Gao, W. Li, et al., J. Med. Chem. 65 (2022) 10534–10553.
[29] G. Poce, S. Consalvi, G. Venditti, et al., ACS Med. Chem. Lett. 10 (2019) 1423–1429.
[30] S. Zhang, Z. Xu, C. Gao, et al., Eur. J. Med. Chem. 138 (2017) 501–513.
[31] A. Sharma, A.K. Agrahari, S. Rajkhow, et al., Eur. J. Med. Chem. 238 (2022) 114454.
[32] P.Z. Zhang, S.F. Zhou, T.R. Li, et al., Chin. Chem. Lett. 23 (2012) 1381–1384.
[33] J.N. Sangshetti, F.A.K. Khan, R.S. Chouthe, et al., Chin. Chem. Lett. 25 (2014) 1033–1038.
[34] P. Thirumurugan, D. Matosiuk, K. Jozwiak, et al., Chem. Rev. 113 (2013) 4905–4979.
[35] A.K. Agrahari, P. Bose, M.K. Jaiswal, et al., Chem. Rev. 121 (2021) 7638–7956.
[36] W.C. Tseng, L.Y. Wang, T.S. Wu, et al., Tetrahedron 67 (2011) 5339–5345.
[37] L. Collins, S.G. Franzblau, Antimicrob. Agents Chemother. 41 (1997) 1004–1009.
[38] O.K. Onajole, M. Pieroni, S.K. Tipparaju, et al., J. Med. Chem. 56 (2013) 4093–4103.
[39] R. Ramesh, D.S. Reddy, J. Med. Chem. 61 (2017) 3779–3798.
[40] S. Lun, H. Guo, O.K. Onajole, et al., Nat. Commun. 4 (2013) 2907.
[41] T.R. Ioerger, S. Koo, E.G. No, et al., PLoS One 4 (2009) e7778.
[42] N.N. Wang, J. Dong, Y.H. Deng, et al., J. Chem. Inf. Model. 56 (2016) 763–773.